Ring Current Modeling : Approaches, Status and Outstanding Challenges

Mei-Ching Fok
NASA Goddard Space Flight Center, USA

Contributors: Natasha Buzulukova, Margaret Chen, Yusuke Ebihara, Alex Glocer
Jerry Goldstein, Vania Jordanova, Stan Sazykin, and Sorin Zaharia

2009 GEM Workshop
June 21 – 26, 2009
Snowmass, Colorado

Outline

- **Ring Current**: Key Element in Geospace Modeling
- Ring Current Modeling: **Approaches**
- Ring Current Modeling: **Status**
- Ring Current Modeling: **Outstanding Challenges**

The Earth’s Inner Magnetosphere

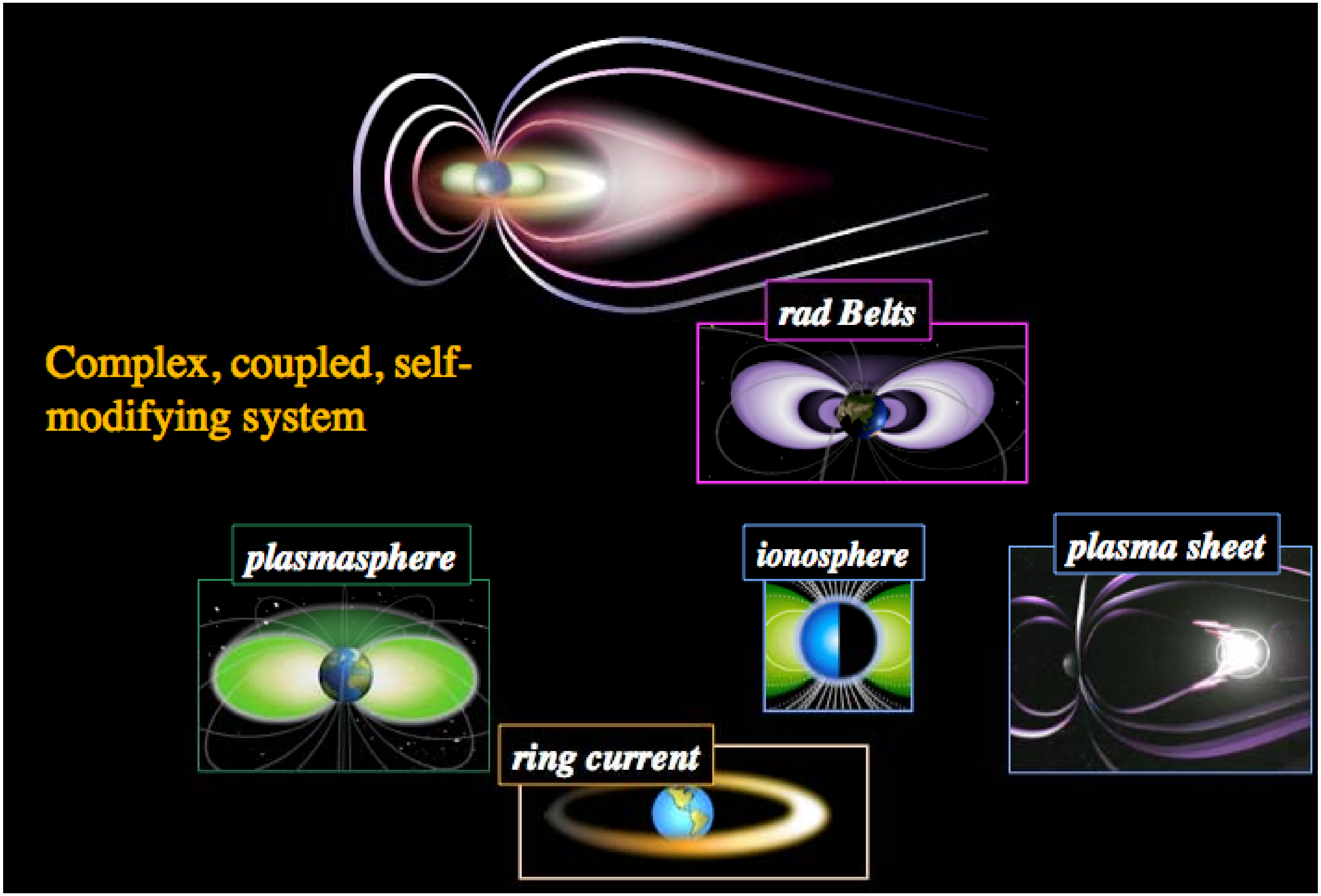

Courtesy of J.Goldstein

Electrodynamics of Ring-Current Ionosphere Coupling

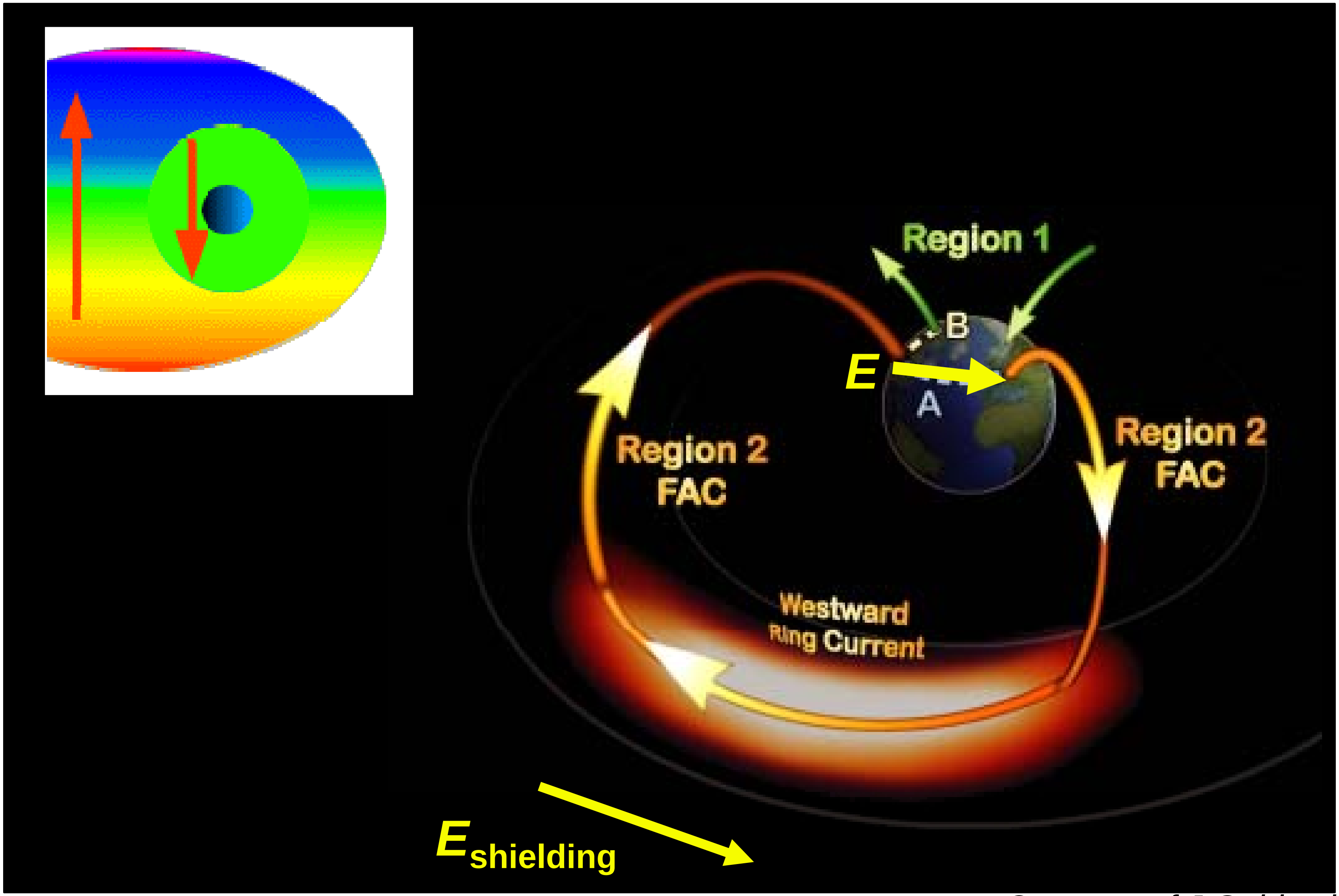

Courtesy of J.Goldstein

Ring Current Effects on the Plasmasphere

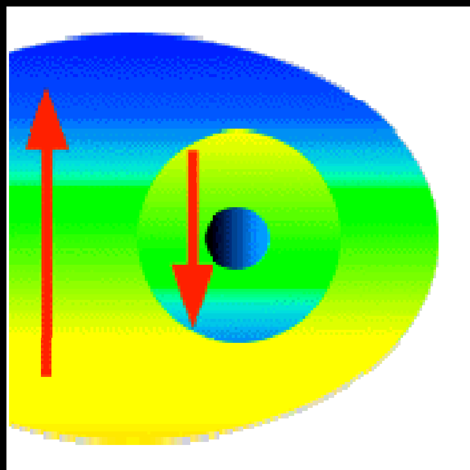

Overshielding

IMAGE EUV

[Goldstein et al., 2002]

Courtesy of J.Goldstein

Ring Current Effects on the Radiation Belts

Simulated Radiation Belt Electron Flux (2 – 6 MeV)
by the Radiation Belt Environment (RBE) Model

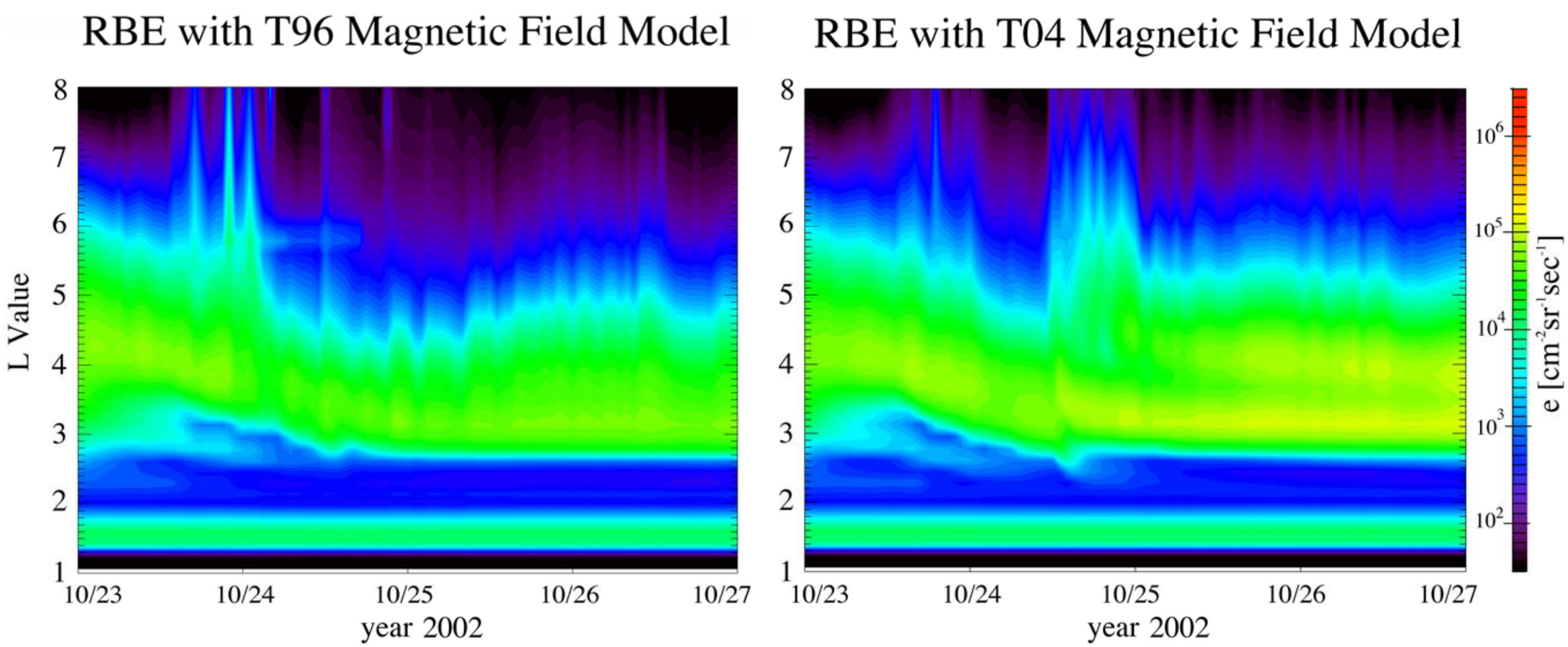

Fok et al., 2008

Ring Current Effects on the Global Magnetosphere

Global MHD
(BATSRUS)

Global MHD + Ring Current
(BATSRUS+RCM)

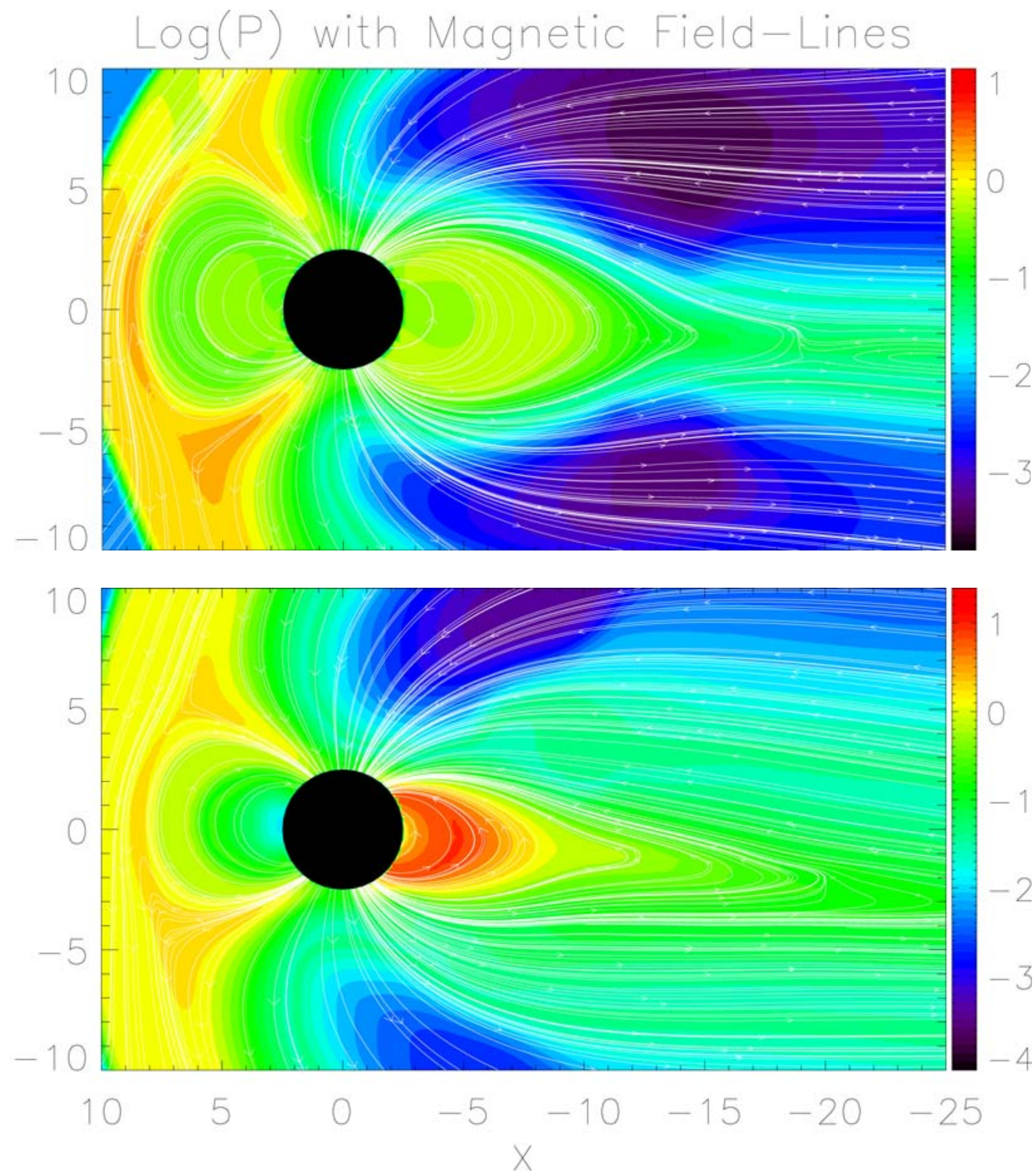

Courtesy of A. Glocer

Ring Current Modeling: Approaches

- Guiding Center Simulation (e.g., M. Che

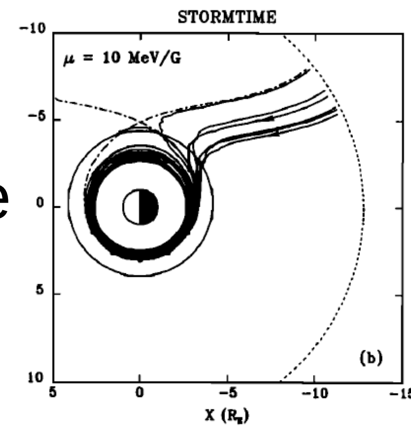

- Kinetic Approach (e.g., RCM, RAM, CRCM)

$$\frac{\partial f}{\partial t} + \vec{v} \cdot \frac{\partial f}{\partial \vec{r}} = \left(\frac{\delta f}{\delta t}\right)_{\text{loss}} + \left(\frac{\delta f}{\delta t}\right)_{\text{diffusion}}$$

- In RAM, $f = Q\ (E, \alpha_o)$ and in CRCM, $f = f\ (\mu, J)$, phase space density

- In RCM, $f = \eta\ (\lambda)$, number of particles per magnetic flux

Electric Field in Ring Current Simulation

- Analytical Models: Volland-Stern, Ensemble of decaying impulses, …
- Empirical Models: Weimer, McIlwain, …
- Data Assimilation Models: AMIE, …
- MHD Electric Field: BATSRUS+Fok, …
- Self-consistent Models:
  - Rice Convection Model (RCM)
  - Comprehensive Ring Current Model (CRCM)
  - Ring Current-Atmosphere Interaction Model (RAM+IE module)

Self-Consistent Electric Field – Vasyliunas Loop

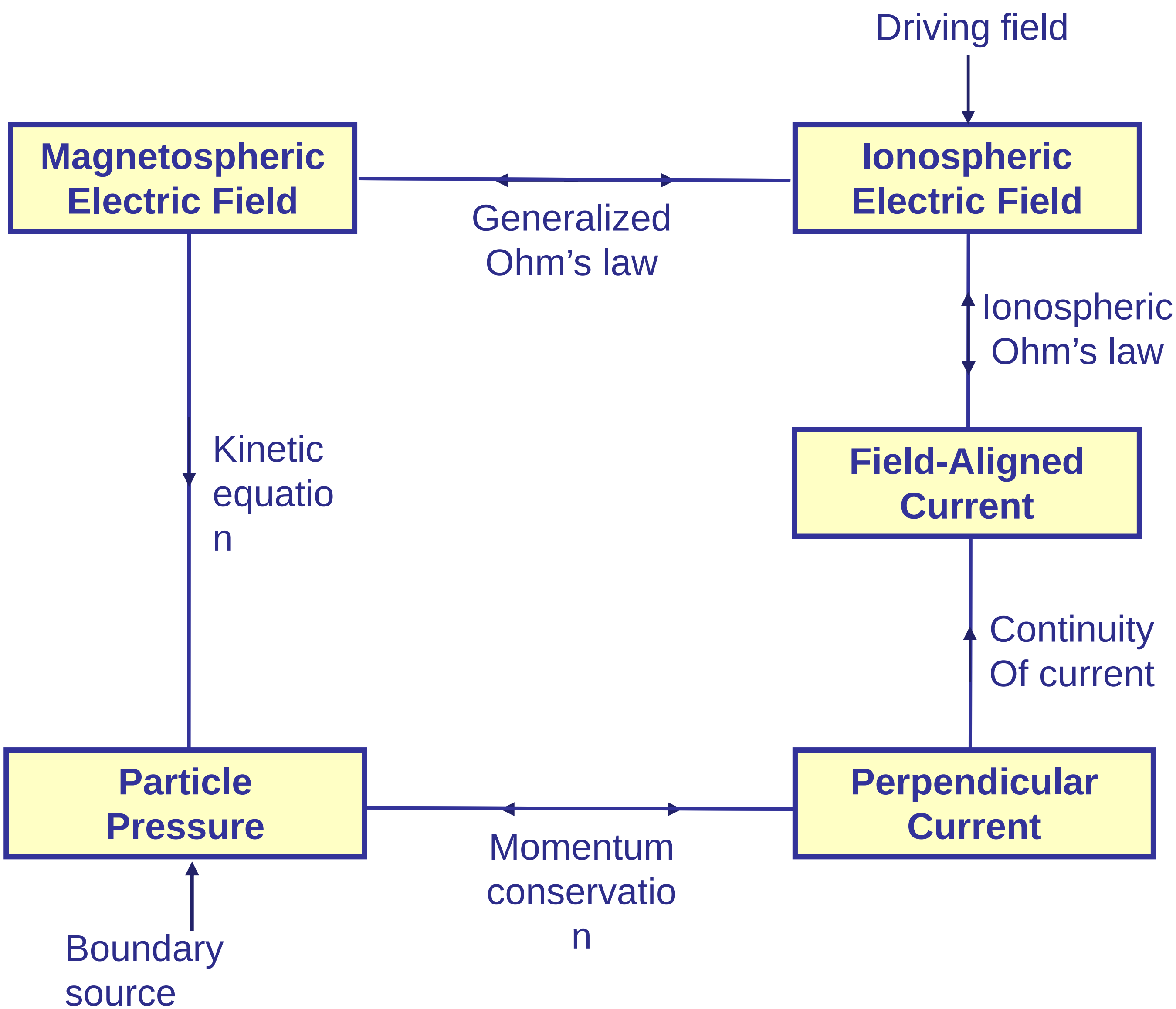

Importance of Realistic $J_{||}$ in M-I Coupling

Buzulukova et al., 2009

No corotation | With corotation

BATSRUS-IE output:
equatorial electric field

(FOK-BATSRUS)

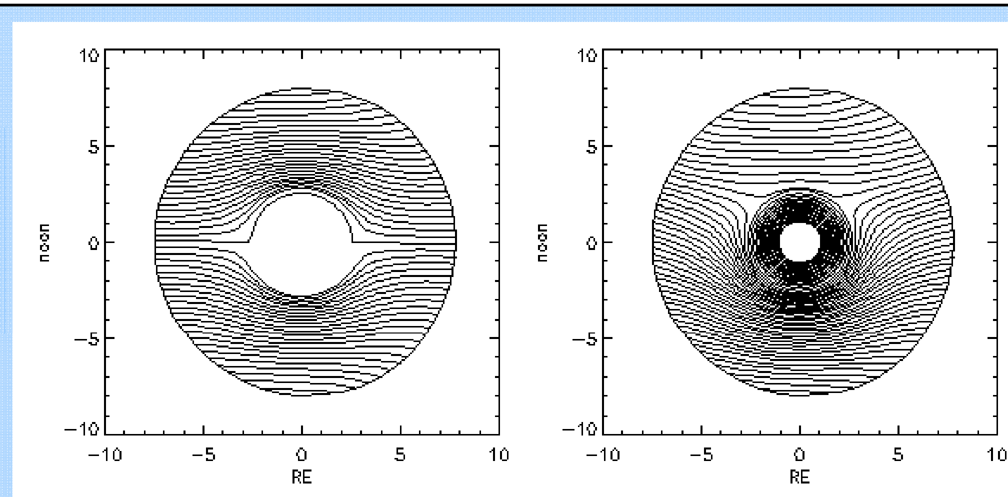

BATSRUS-IE output at CRCM polar boundary only

(CRCM-BATSRUS)

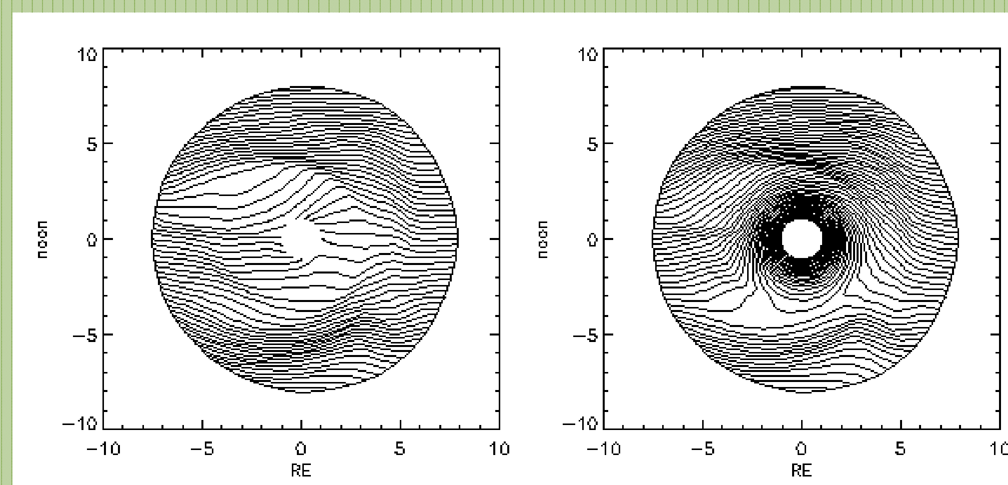

Self-consistent **E** Reproduces IMAGE/HENA Data

IMAGE HENA data **CRCM+BATSRUS**

07 UT
Aug 12, 2000

60-119 keV H

27-39 keV H

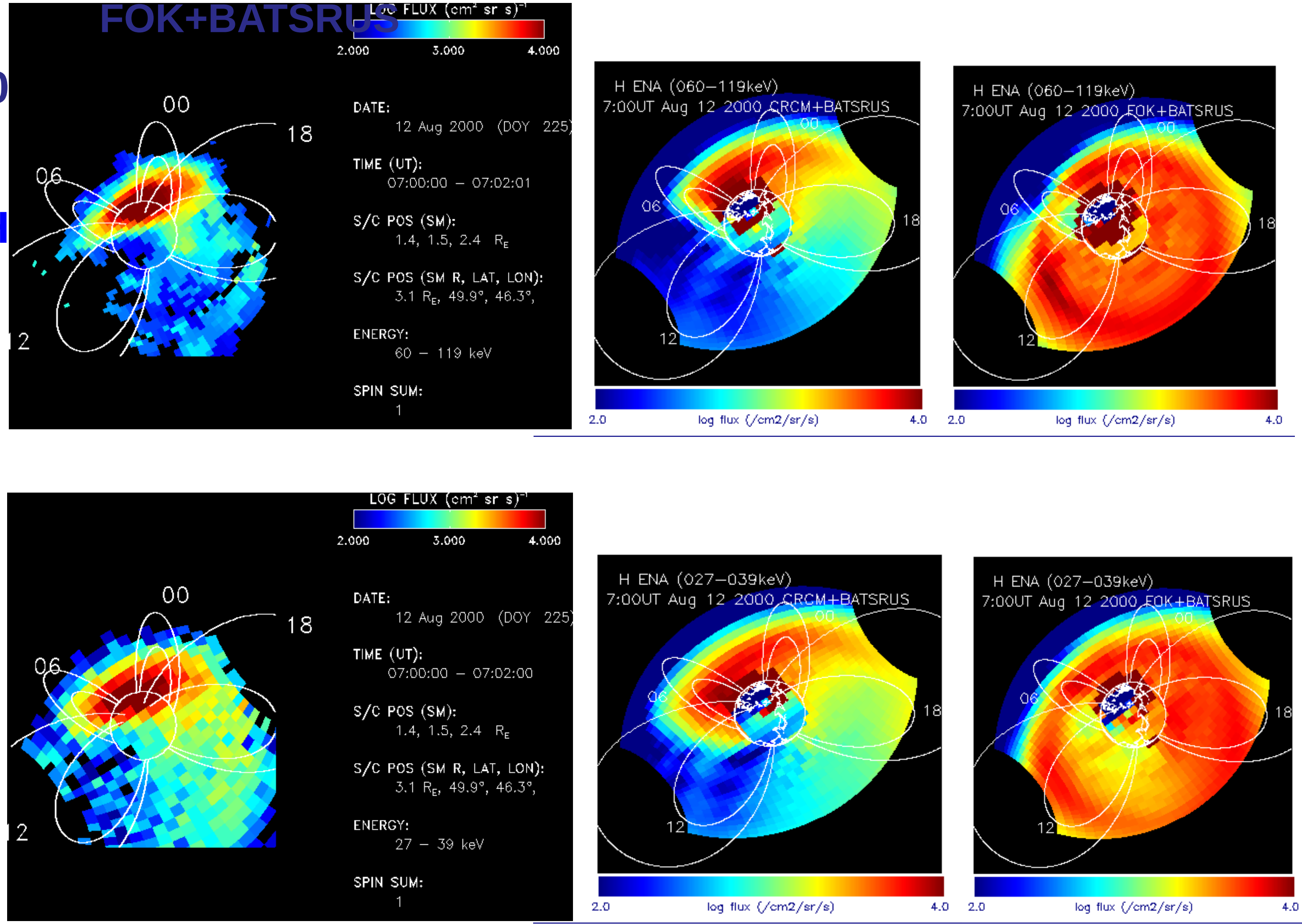

Buzulukova et al., 2009

The TWINS Mission

Two **W**ide-angle **I**maging **N**eutral-atom **S**pectrometers

First Stereoscopic Magnetospheric Imaging Mission
TWINS proposed in 1997, MoO (AO 97-OSS-03)
2 nadir-viewing Molniya-orbit spacecraft
7.2 RE apogee, 63.4˚ inclination, 12 hour orbit
Actuator replaced S/C spinning

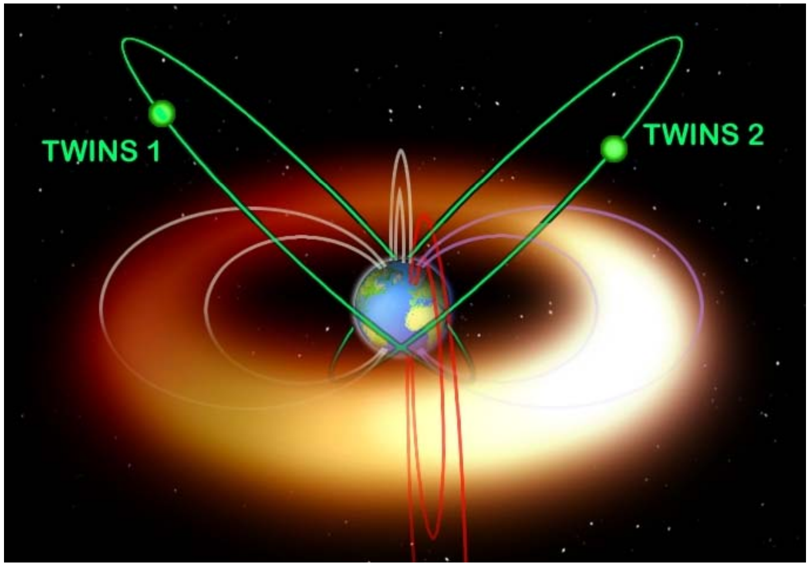

Stero Imaging began in summer of 2008
Available at http://twins.swri.edu

TWINS Team:
PI: Dave McComas (SwRI)
Project Scientist: Mei-Ching Fok (NASA)
Program Scientist: Barbara Giles (NASA)
Science Analysis Lead: Jerry Goldstein (Sw

TWINS 1 / TWINS 2 - CRCM Data-model comparison: stereoscopic view (12 keV) at ~10:30 UT (main phase)

TWINS 1

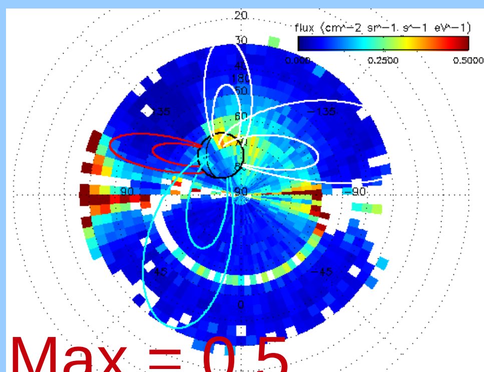

Max = 0.5

TWINS 2

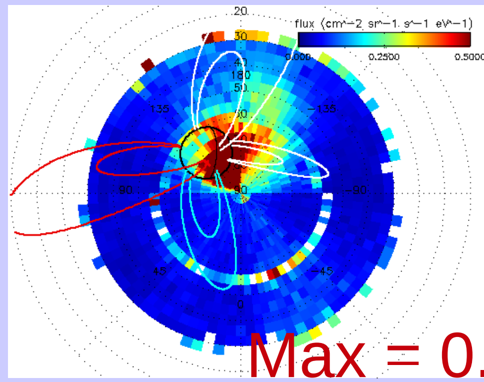

Max = 0.5

CRCM ENA

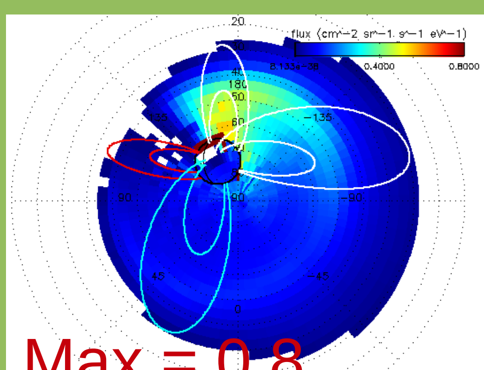

Max = 0.8

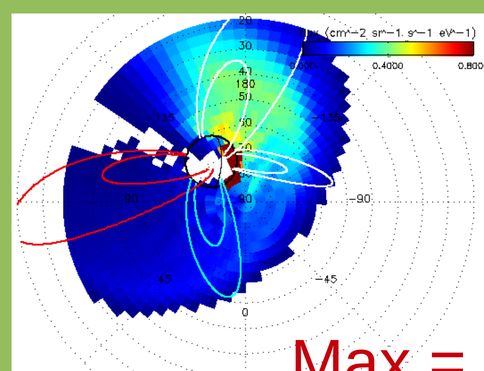

Max = 0.8

12 keV H+ flux

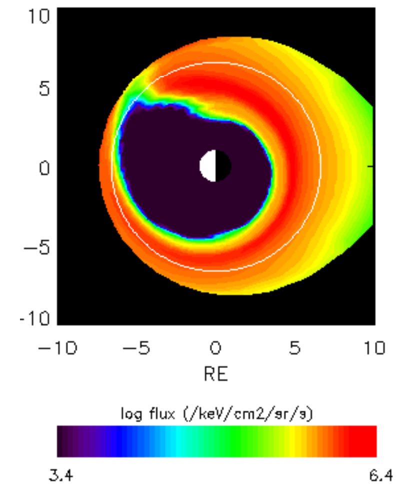

Total RC pressur

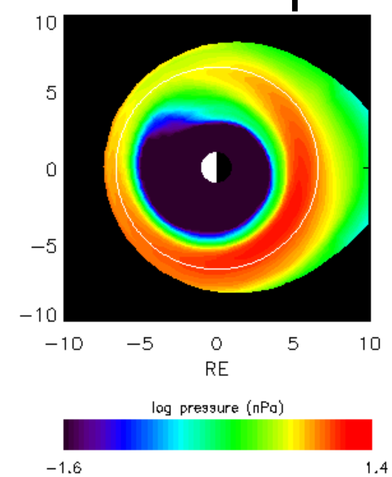

Magnetic Field in Ring Current Simulation

- Dipole
- Dipole + southward ΔB
- Empirical models: Tsyganenko, Hilmer-Voigt, …
- Global MHD Models: BATSRUS, LFM, OpenGGCM, …
- Self-consistent Models:

  - MHD with feedback of ring current pressure (BATSRUS+RCM, …)

  - Force Balance: $\mathbf{J}\times\mathbf{B} = -\nabla\cdot\mathbf{P}$ (RCM-E, RAM-SCB, ECRCM, …)

RAM-Self-consistent B (RAM-SCB)

Ring current-atmosphere interactions model (RAM)

[Jordanova et al., 1994, 2006]

- Bounce-avg. Boltzmann eq.
- Convective/corotation E-field (empirical)
- Updated to general B

Pressure →

← B-field

3D equilibrium code

[Cheng, 1995; Zaharia et al., 2004]

$$\mathbf{J} \times \mathbf{B} - \nabla \cdot \mathbf{P} = 0$$

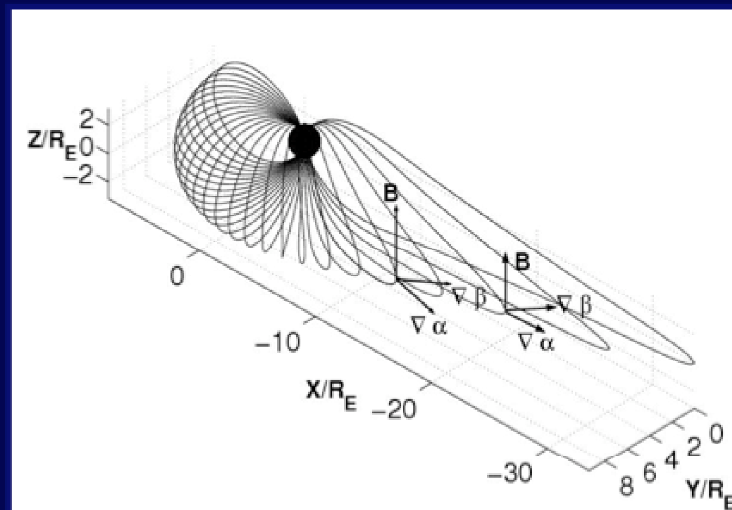

- Euler potentials (flux coordinates)
- Empirical B-field BCs

Los Alamos NATIONAL LABORATORY EST. 1943

Plasma Pressure

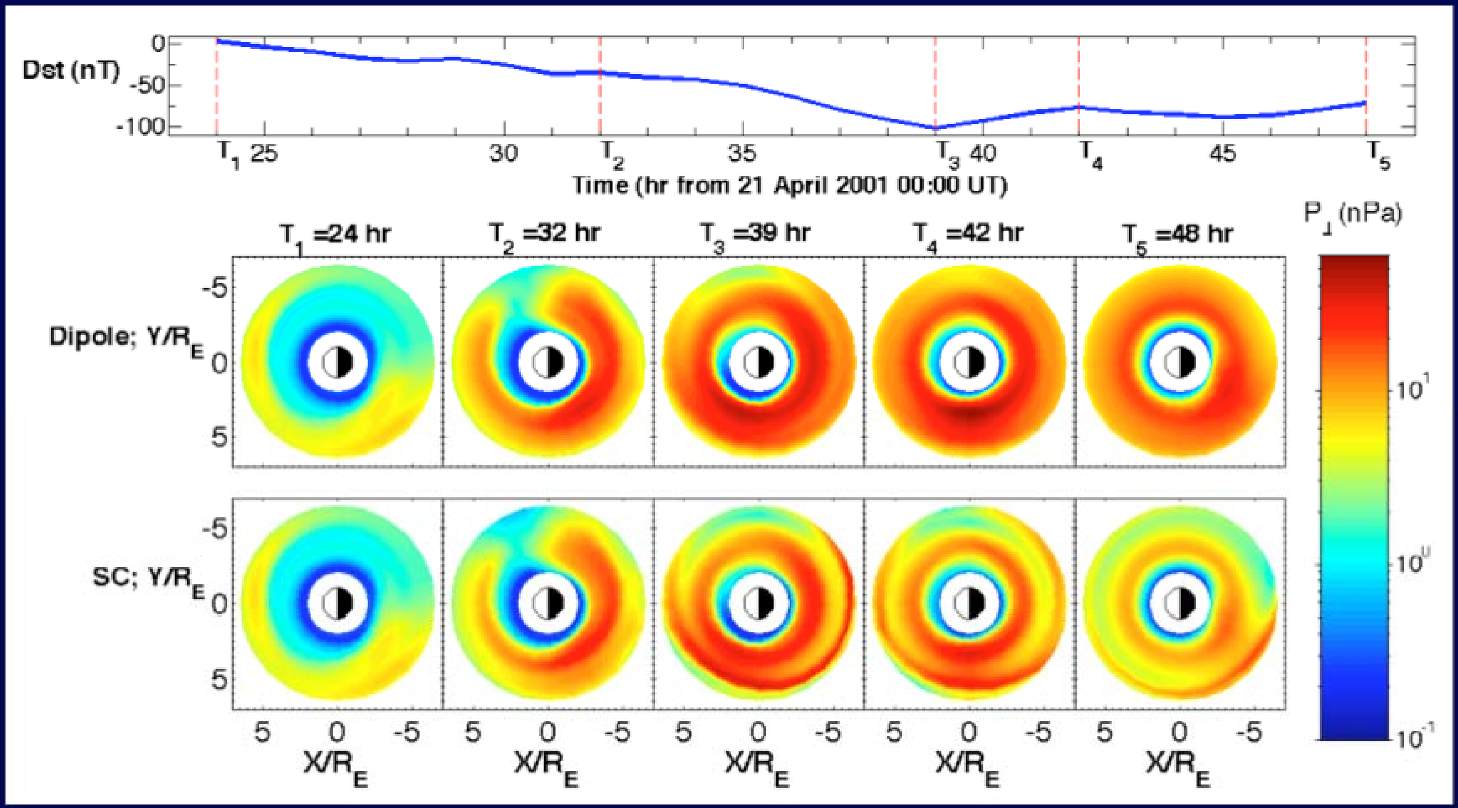

From *Zaharia et al., [2006]*

- Lower (~ ½) pressure in SC case than in run with dipole field; magnetic self-consistency/stretching of the B-field reduces the injected ring current energy density

Extended Comprehensive Ring Current Model (ECRCM)

(1) Start at *t0* with a magnetic field configuration, **B0**. Set **B** = **B0**

(2) For given particle pressure distribution, calculate the perpendicular current, $\mathbf{J}_\perp$

$$\mathbf{J}_\perp = \frac{\mathbf{B}}{B^2} \times \left[\nabla P_\perp + \left(P_\parallel - P_\perp\right) \frac{(\mathbf{B}\cdot\nabla)\mathbf{B}}{B^2} \right]$$

(3) Calculate **dB** from integrating $\mathbf{J}_\perp$ using the Biot-Savart law:

$$\mathbf{dB}(\mathbf{r}) = \frac{\mu_o}{4\pi} \int \frac{\mathbf{J}_\perp(\mathbf{r}') \times (\mathbf{r} - \mathbf{r}')}{|\mathbf{r} - \mathbf{r}'|^3} d^3 r'$$

(4) Update **B** with **B** = **B0** + **dB.** Repeat step (2) to (4) until **B** reaches convergence:

$$\frac{\sum \left|\nabla \cdot \vec{P} - \mathbf{J}_\perp \times \mathbf{B}\right|}{\sum \left|\nabla \cdot \vec{P} - \mathbf{J}_\perp \times \mathbf{B}\right|_{\mathbf{B=B0}}} < 5\%$$

where the summation is over the model domain of the ring current model.

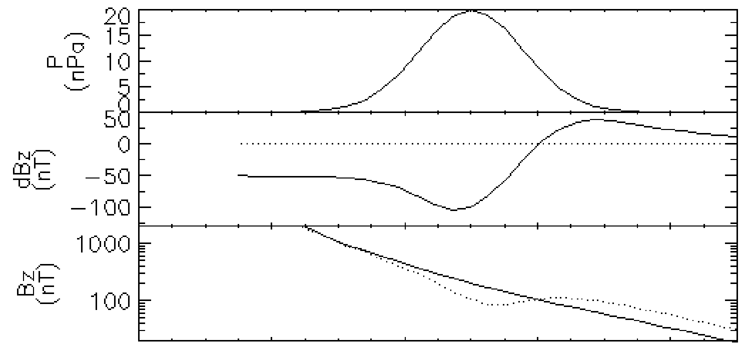

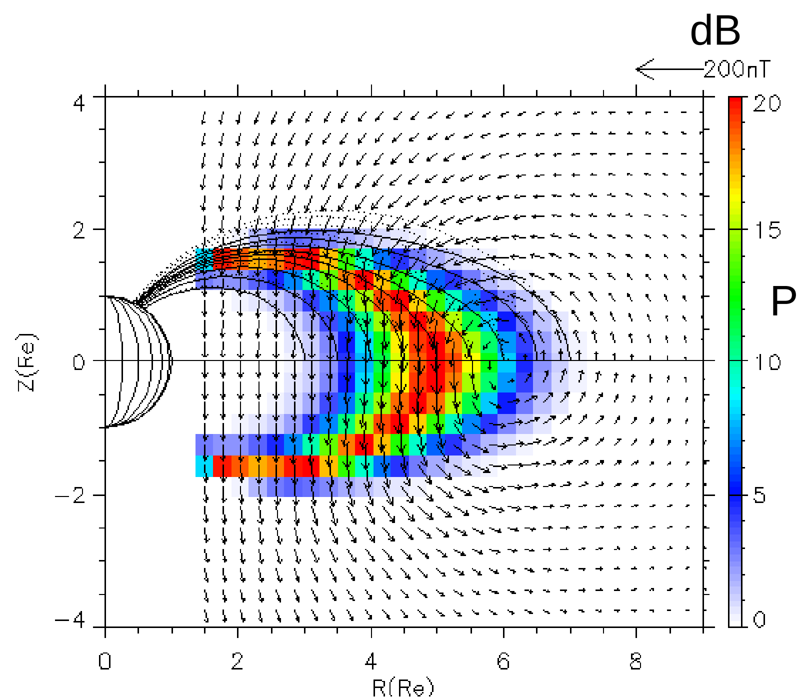

Ebihara et al., 2008

ECRCM Reproduces Butterfly Pitch-Angle Distribution

ECRCM Calculation

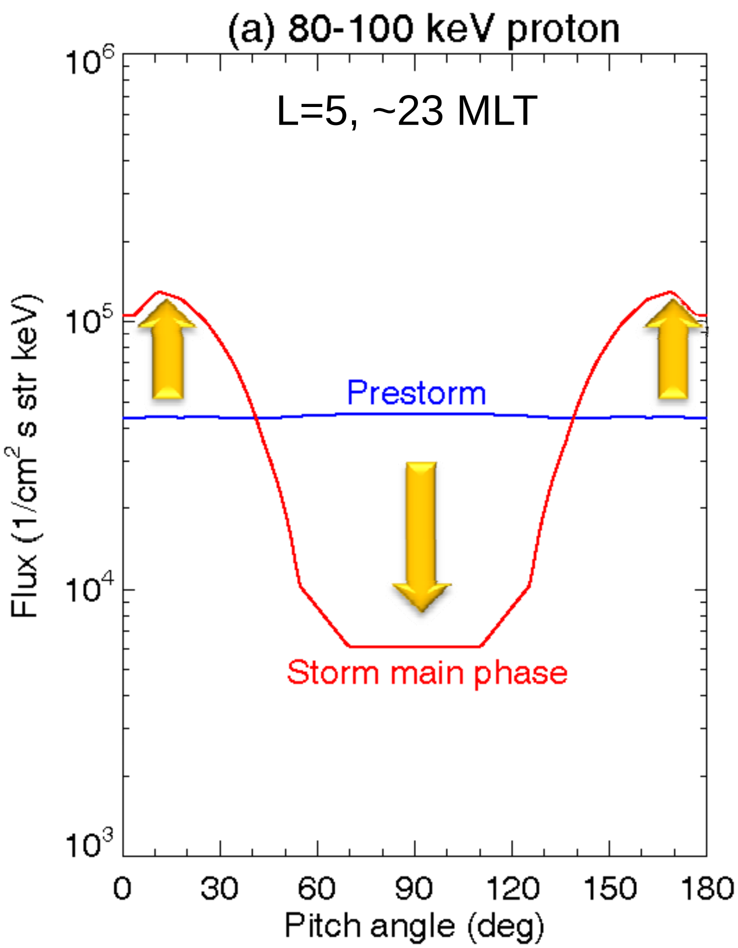

Polar/MICS Observation

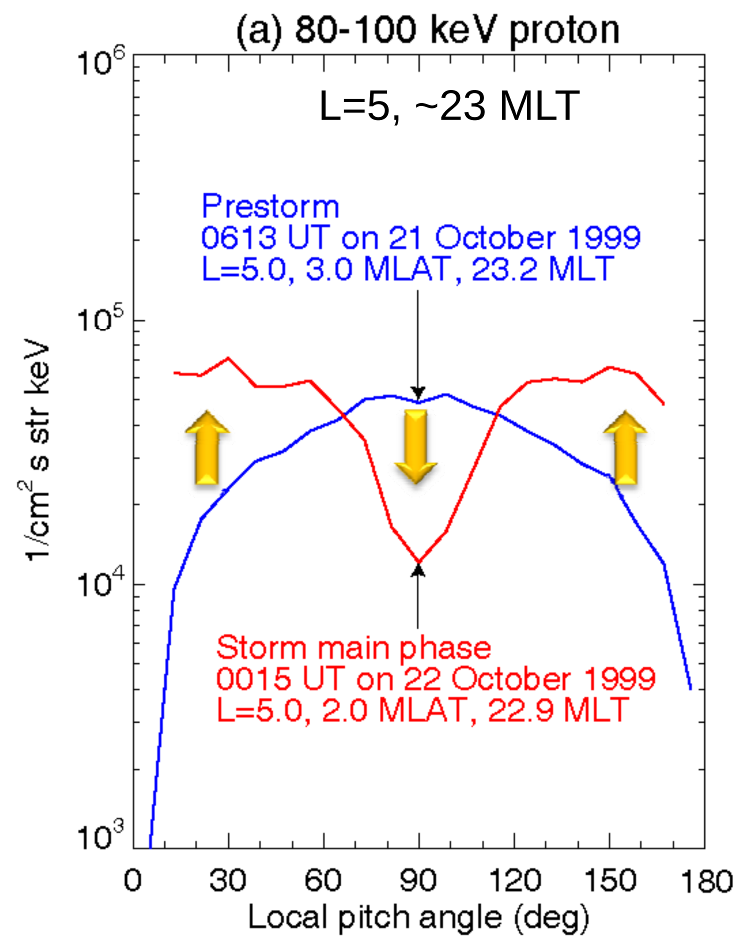

- Proton flux at ~90 deg decreases due to adiabatic deceleration to conserve ❍
- Flux aligned flux increases due to adiabatic acceleration to conserve *J*

Boundary Conditions in Ring Current Simulation

- Data: LANL geosynchronous satellites, Geotail, …
- Empirical models: Maxwellian or kappa dist. with *n* and *T* from models of Tsyganenko-Mukai, Ebihara and Ejiri, Borovsky…
- Time-independent Model: constant *n* and *T*
- Temperature and density from MHD output
- Test-particle calculations of H^+ and O^+: Fok et al., 1999, 2006

Time-Varying B. C. in Simulating a Major Storm

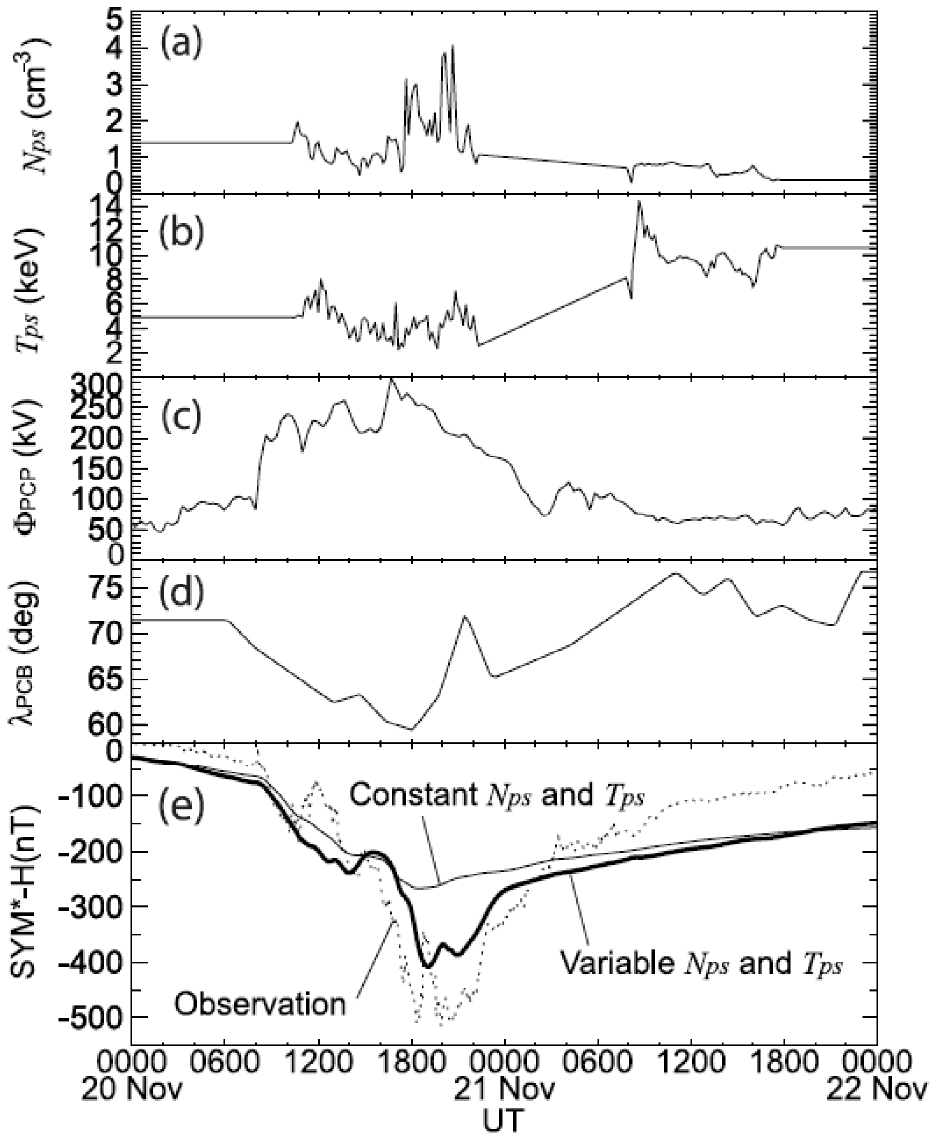

- CRCM simulation of November 20-22 2003 storm
- 2 Runs: (1) Time-varying boundary condition given by LANL satellites at L=6.6, (2) Constant *Nps* = 1 cm-3 and *Tps* = 5 keV
- CRCR run with time-varying boundary condition has much better predicted symH*

Ebihara et al., 2005

Interchange Instability Caused by Time-Varying B. C.

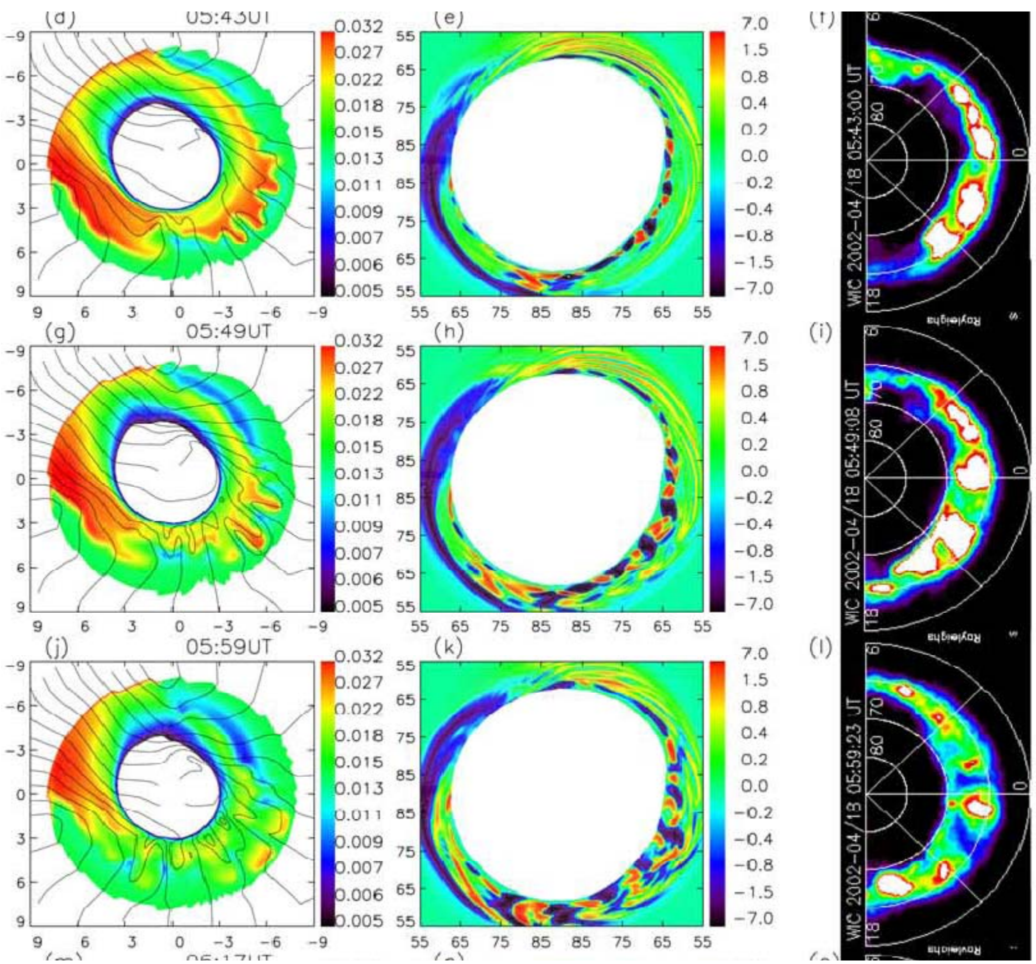

- RCM simulation of April 17-22 2002 storm. Sawtooth “onset” at 5:30 UT
- Time-varying boundary condition given by Geotail data
- Left: Model-predicted $PV^{5/3}$ in the equatorial plane
- Middle: Field-aligned current densities in northern ionosphere
- Right: IMAGE FUV/WIC auroral images (data courtesy of H. U. Frey

Courtesy of A. Sazykin

Pre-conditioning of Plasma Sheet Before Storm

From 10-yr averaged Geotail data [Wang *et al.*, *JGR*, 2007]

CONDITION 1

Strongly Northward IMF

high solar-wind N

low solar-wind v_x

highest N and lowest T: in the post-midnight sector

CONDITION 2

Weakly Northward IMF

low solar-wind N

high solar-wind v_x

lowest ion N and highest T: in the pre-midnight sector

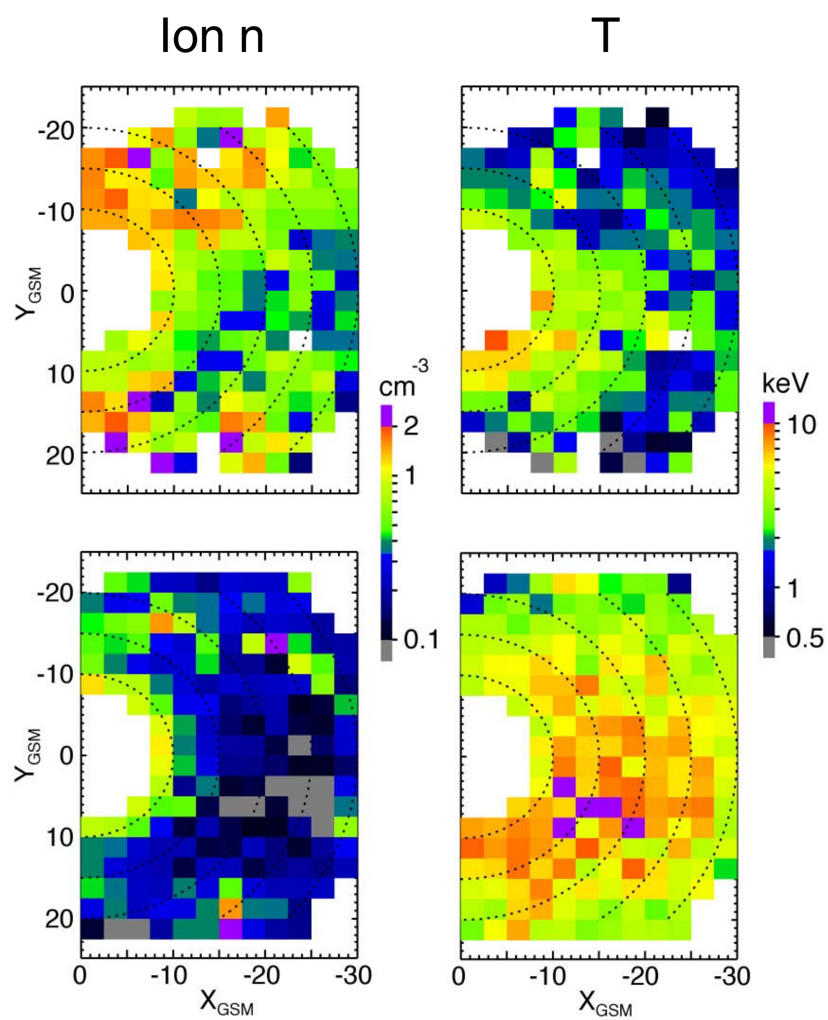

From [Chen *et al.*, *GRL*, 2007]

Cold Dense Plasma Sheets Leads to Intense Ring Current

Equatorial Perpendicular Pressure at $R_0 = 4.2$

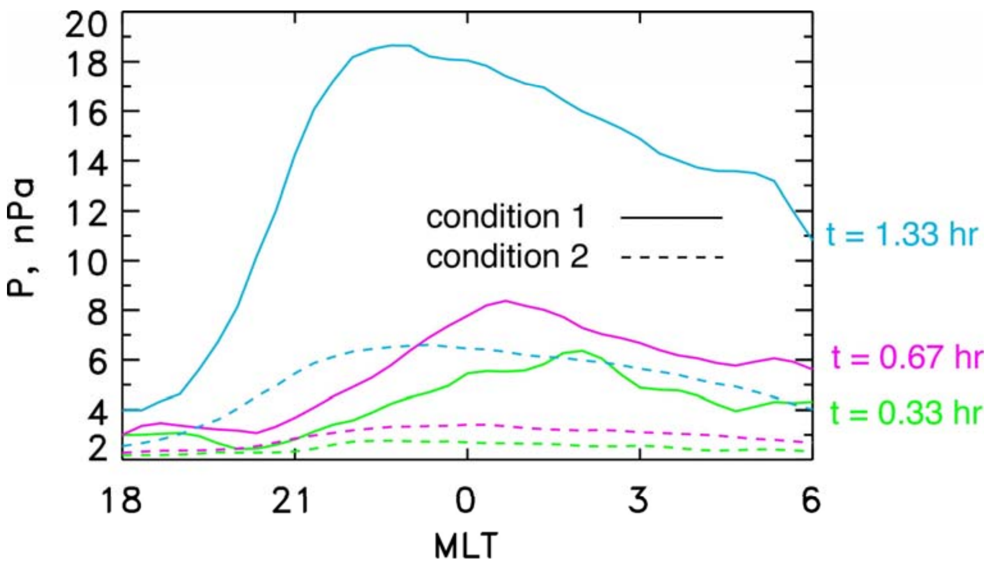

From [Chen *et al.*, *GRL*, 2007]

- Applied Geotail ion data as boundary conditions to a magnetically self-consistent ring current simulation.
- Condition 1 (cold dense plasma sheet) leads to an overall more intense ring current than condition 2. This is consistent with findings of Lavraud *et al*. [2006].

- Early (~ first 40 min) in the storm main phase,
  - Condition 1 (cold dense) leads to a stronger enhancement in the simulated ring current perpendicular pressure distribution in the post midnight sector than condition 2.
  - Condition 2 (hot tenuous) leads to a weaker and azimuthally more nearly uniform enhancement of P on the night side than condition 1.

Boundary Distribution by Test-Particle Calculation

n and *T* at CRCM boundary

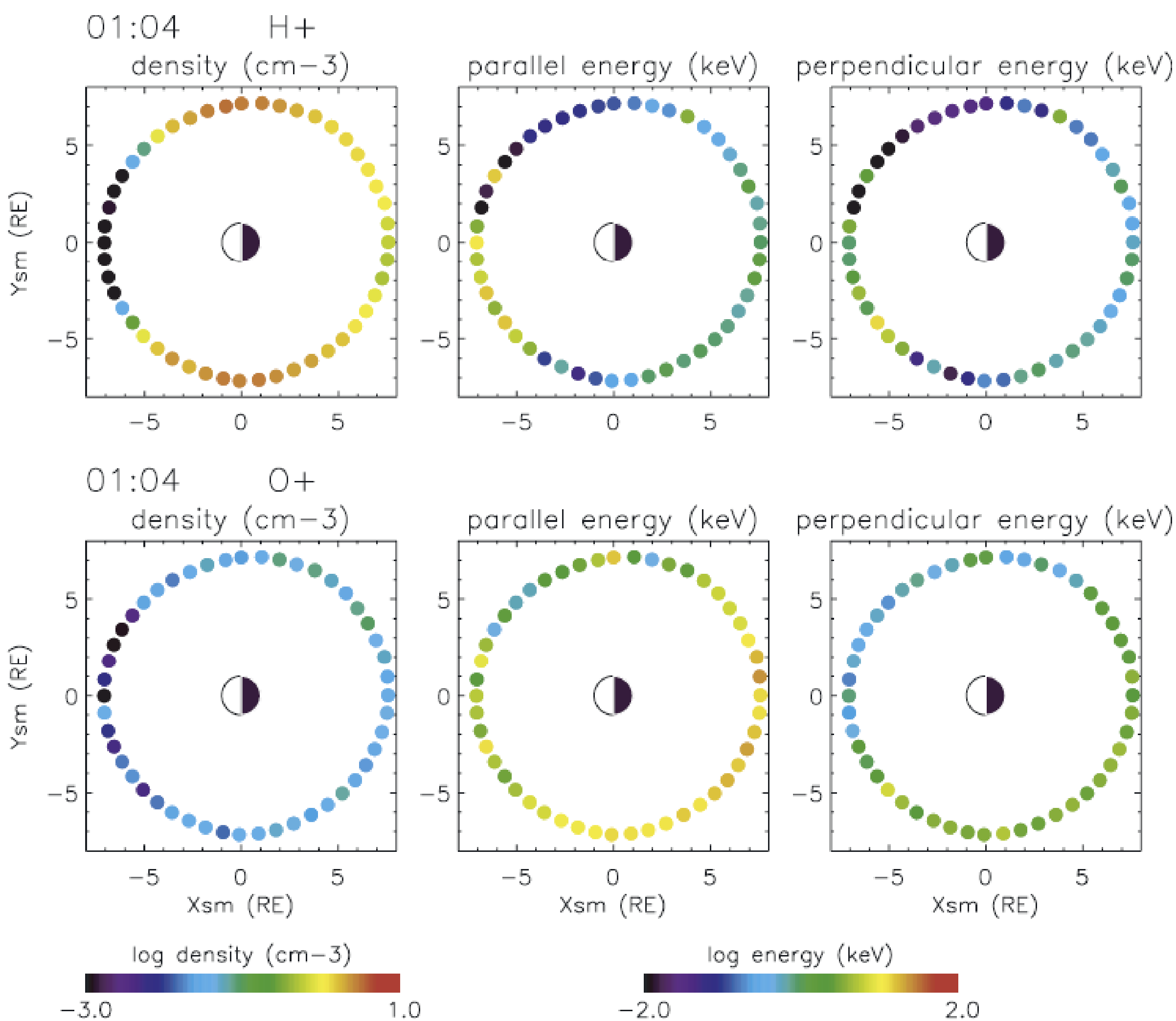

- Test-particle calculation of ions from the solar wind and ionosphere during a substorm
- Higher O^+ energy at 8 RE
- O^+ Epar > Eper during substorm

Fok et al., 2006

Model the Decay of the Ring Current

$$\frac{\partial f}{\partial t} + \vec{v} \cdot \frac{\partial f}{\partial \vec{r}} = \left(\frac{\delta f}{\delta t}\right)_{\substack{\text{charge}\\\text{exchange}}} + \left(\frac{\delta f}{\delta t}\right)_{\substack{\text{Coulomb}\\\text{collision}}} + \left(\frac{\delta f}{\delta t}\right)_{\text{losscone}} + \left(\frac{\delta f}{\delta t}\right)_{\substack{\text{pitch-angle}\\\text{diffusion}}}$$

Four major loss processes:

- Drift loss at dayside magnetopause
- Charge exchange with neutral atmosphere
- Coulomb Collision with the plasmasphere
- Losscone loss
- Pitch-angle diffusion by wave-particle interactions

Ring Current Drift Loss at Dayside Magnetopause

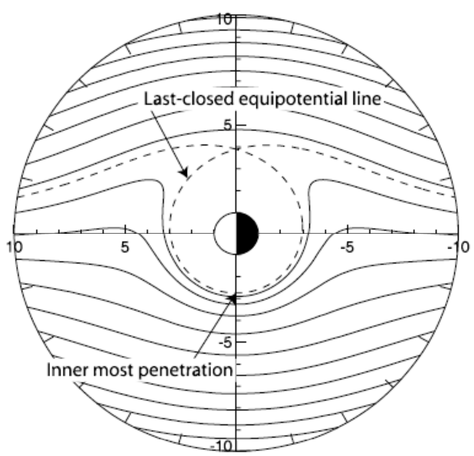

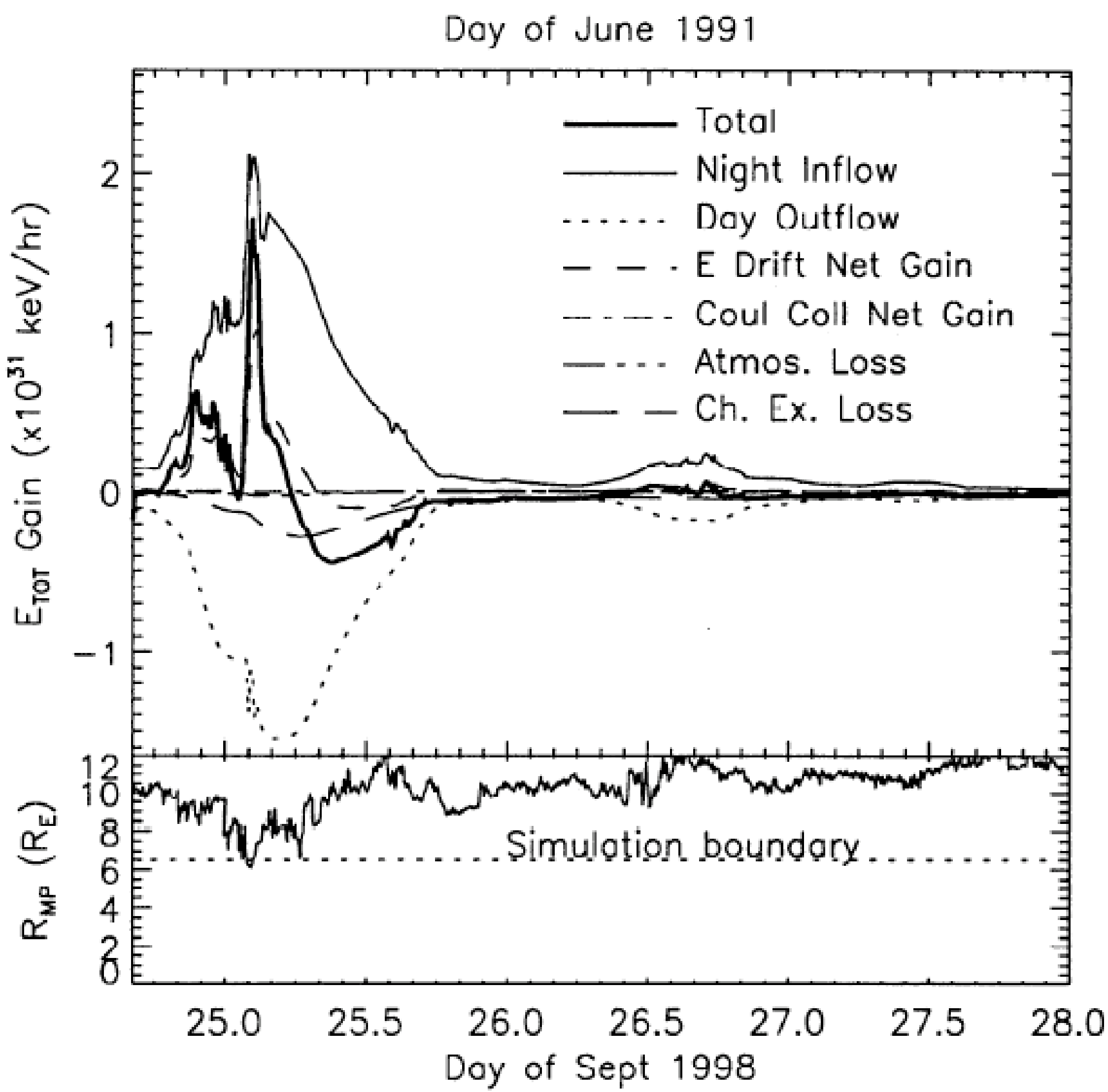

Liemohn et al., 1999

Charge-Exchange Loss of Ring Current Ions

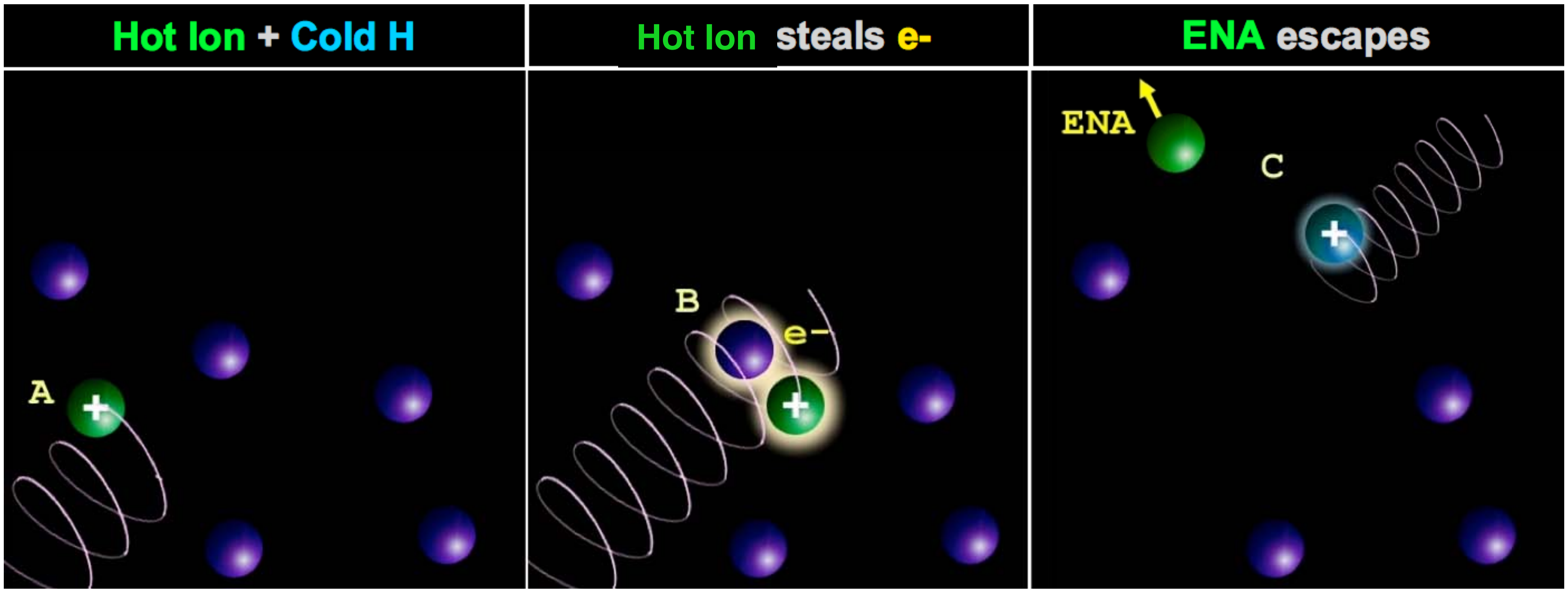

Courtesy of J.Goldstein

$$\frac{\partial f}{\partial t} = -\frac{f}{\tau}, \quad \tau = \frac{1}{\mathrm{v}\sigma n_H}$$

At L ~ 3, ♦ in hours for 10 keV H^+ and days for 100 keV H^+

♦ in days for 10 keV O^+ and hours for 100 keV O^+

Ring Current Coulomb Interaction with Plasmasphere

$$\frac{dE}{dt} = -\frac{m_s \Gamma_s}{v} \sum_b < n_b > Z_b^2 \left[2x^2 \left(1 + \frac{m_s}{m_b} \right) G(x) - erf(x) \right]$$

H$^+$

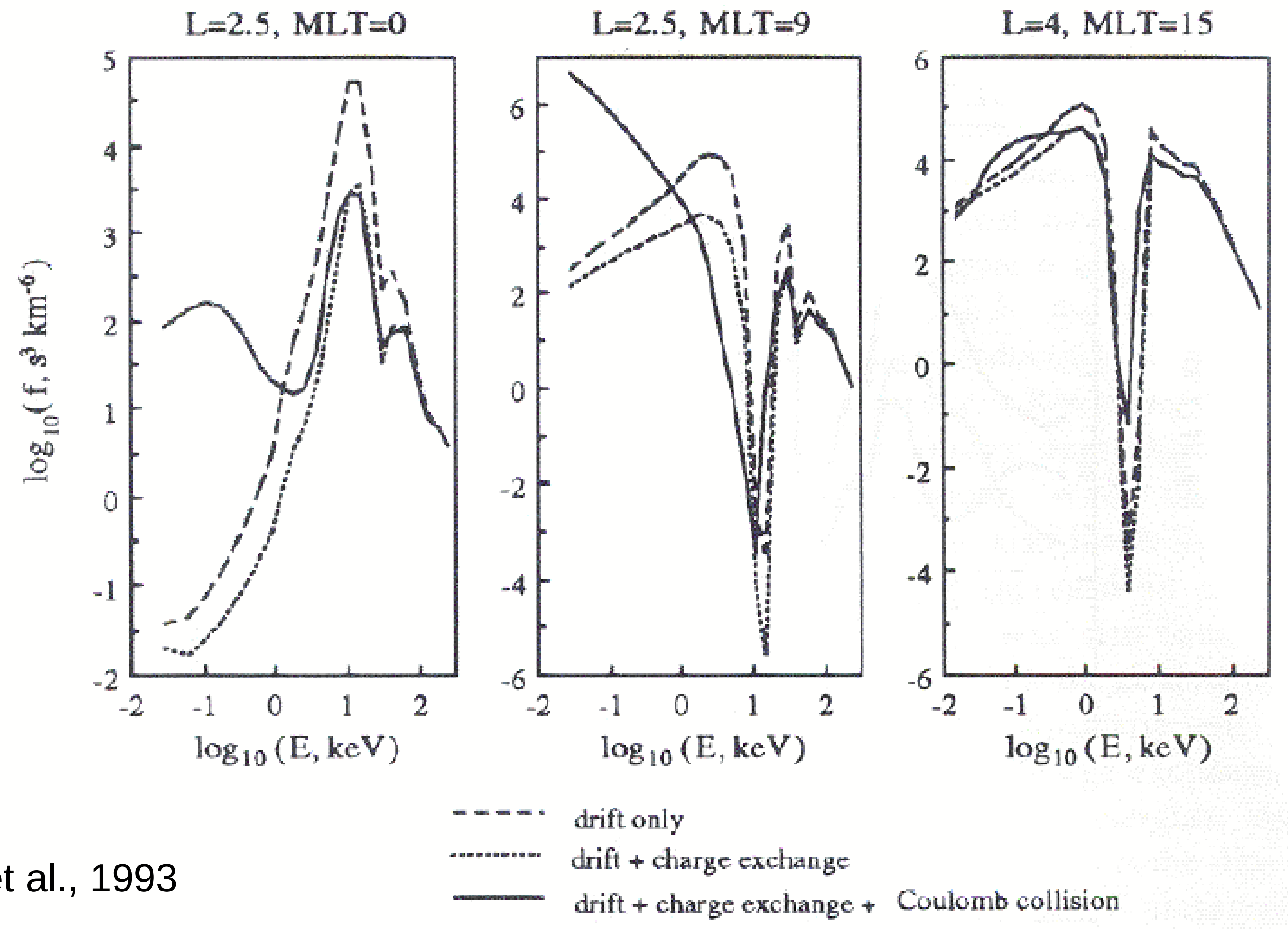

Fok et al., 1993

EMIC-Waves Associated Ring Current Precipitation and Proton Aurora

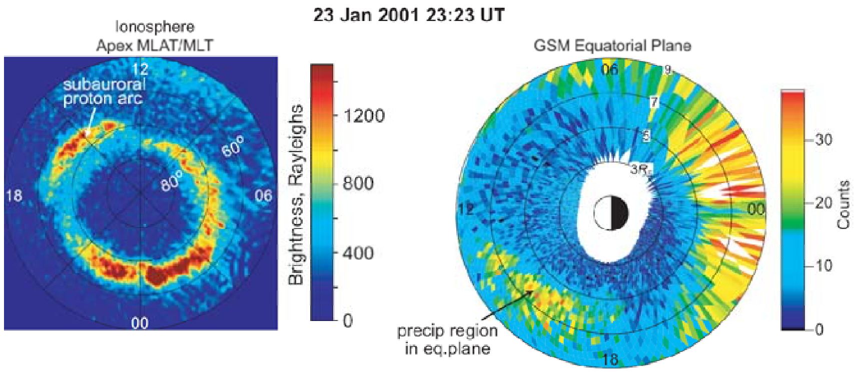

- Images from the **IMAGE/FUV** proton channel mapped to the GSM equatorial plane showing a detached subauroral proton arc on 23 Jan 2001
- Simulations with **RAM** indicating enhancement of **EMIC waves** within regions of spatial overlap of energetic ring current protons and dayside plasmaspheric plumes and along the plasmapause
- The location of the **proton precipitation** by EMIC waves matches very well the temporal and spatial evolution of FUV observations

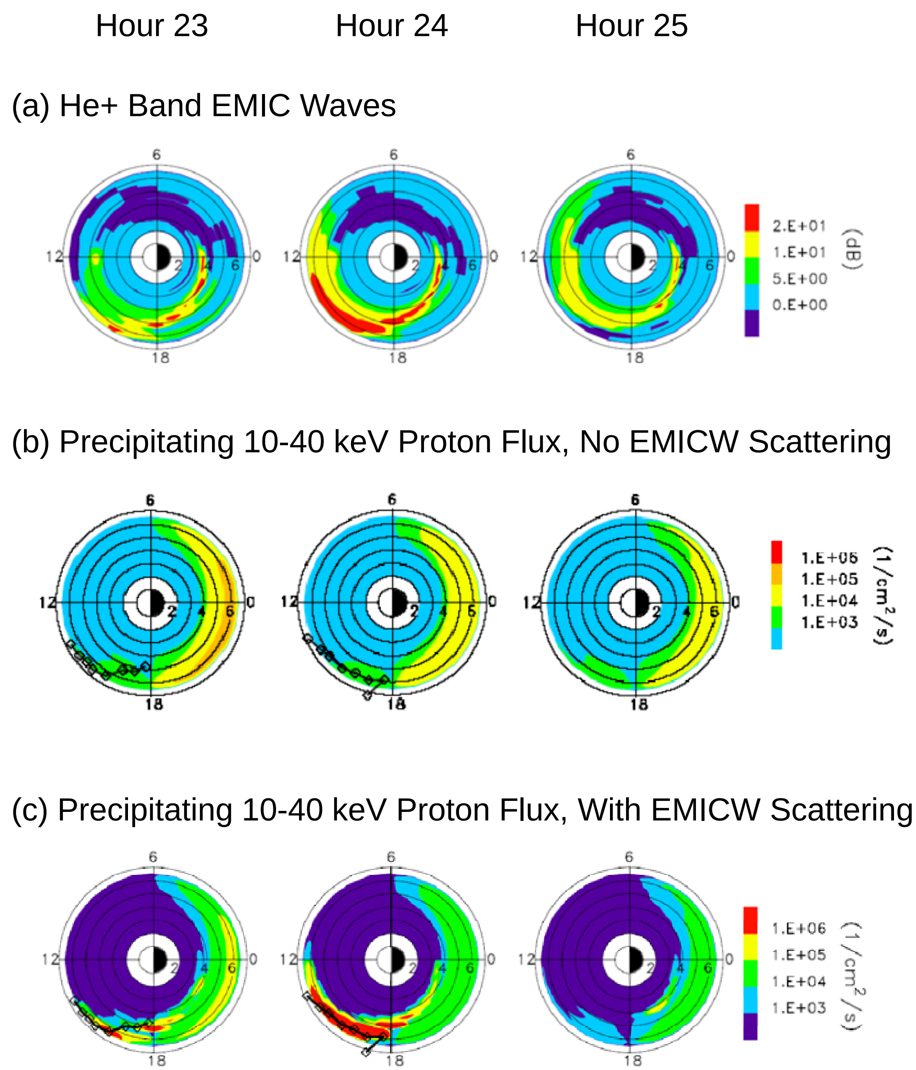

[Jordanova et al., 2007]

Outstanding Challenges in Ring Current Modeling

- Self-consistent **B** and **E** with ring current feedback to global MHD model
- Accurate modeling of the stormtime ring current requires realistic modeling of the pre-storm plasma sheet.
- Ring current composition and ion outflow should be done self-consistently (Ring current with multi-fluid MHD)
- How to model ring current response to substorms (dipolarization and substorm injection)
- Interchange instabilities: physical or numerical? Where and when?
- Combined inner magnetosphere models (ring current, radiation belts, plasmasphere, wave activity) coupled with MHD model, ionosphere electrodynamic and outflow models

Electron Precipitation by EMIC Waves from RAM

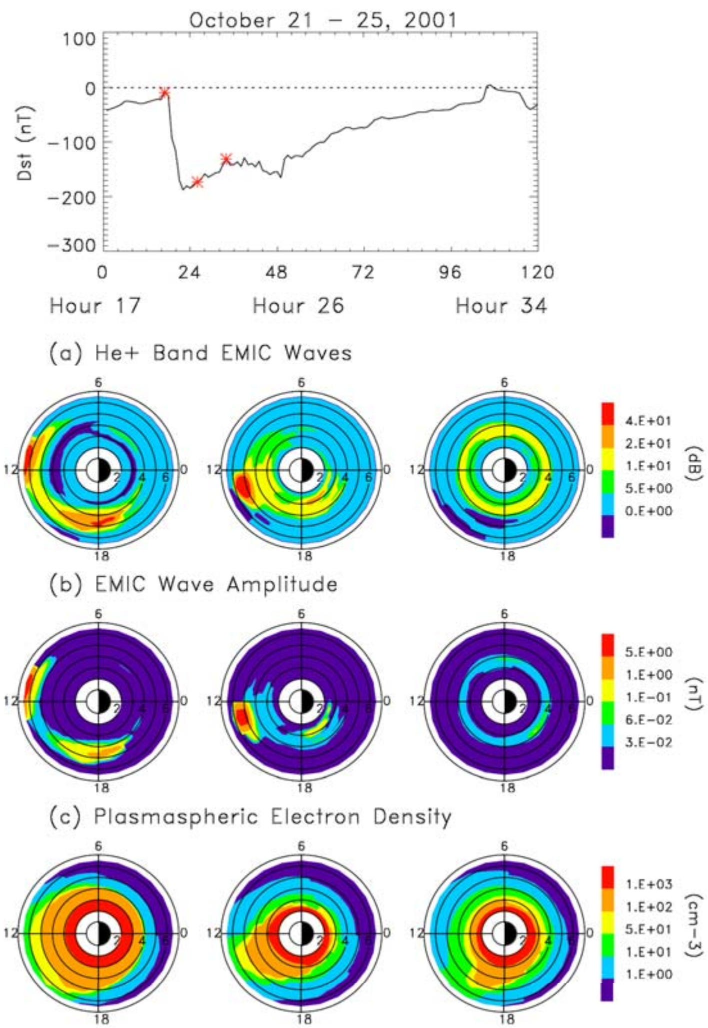

[Jordanova et al., 2008]

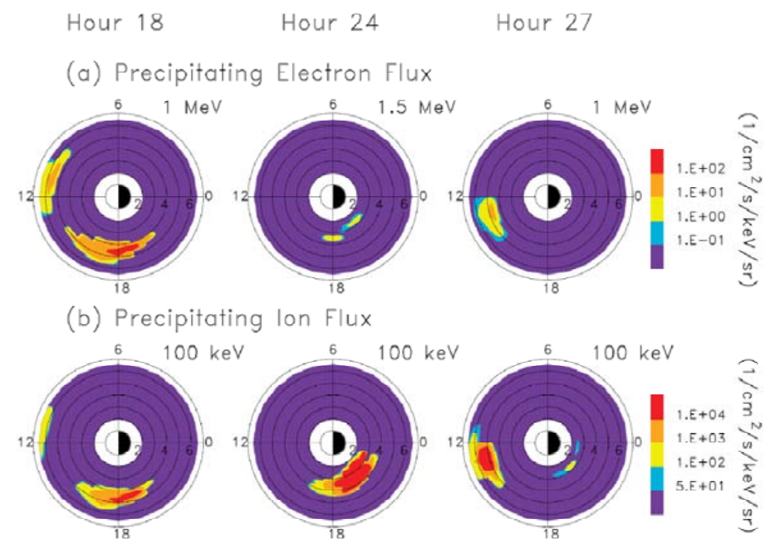

- The excitation of EMIC waves is calculated **self-consistently** with the evolving plasma populations during the October 2001 storm.
- EMIC waves are enhanced within regions of enhanced cold plasma density (plasmaspheric plumes) and along the plasmapause
- **Pitch angle scattering** has large effect within areas of EMIC instability and causes significant loss of radiation belt electrons at E>1MeV
- The precipitating **ion fluxes** are collocated with the precipitating **electron fluxes** but occur at variable energy range and magnitude

Summary

- Kinetic approach in most ring current models
- Recent progress in ring current modeling:

  - RC-MHD coupled codes: self-consistent **E** and **B** and B/C

  - Self-consistent **B** with force balance

  - Boundary conditions reflect history and dynamics of plasma sheet

  - Include ions of solar wind and ionospheric sources:

    RC-multifluid MHD models with ionospheric outflow

  - Coupled inner magnetosphere model – RC+Plasmasphere+RB
- Outstanding challenges:

  - instabilities

  - substorm and fast changes of fields (comparable to bounce period)

  - improve consistency in coupled models